ELSEVIER

Journal of Alloys and Compounds 311 (2000) 130–136

Journal of ALLOYS AND COMPOUNDS

www.elsevier.com/locate/jallcom

Magnetic properties of $Sm(Fe_{1-x}Al_x)_7$ crystals

H. Samata[a], M. Kamonji[b], H. Sasaki[b], S. Yashiro[b], M. Kai[c], T. Uchida[c], Y. Nagata[b,*]

[a]*Faculty of Mercantile Marine Science, Kobe University of Mercantile Marine, Fukaeminami, Higashinada, Kobe 658-0022, Japan*
[b]*College of Science and Engineering, Aoyama Gakuin University, Chitosedai, Setagaya, Tokyo 157-8572, Japan*
[c]*Tokyo Institute of Polytechnics, Iiyama, Atsugi, Kanagawa 243-0297, Japan*

Received 1 June 2000; accepted 19 June 2000

Abstract

$Sm(Fe_{1-x}Al_x)_7$ (x=0, 0.047, 0.07 and 0.12) crystals were grown by the self-flux method, and their crystallographic and magnetic properties were investigated. $Sm(Fe_{1-x}Al_x)_7$ crystallizes in a tetragonal structure of the space group $P4_2/mnm$, and aluminum occupies the iron site. The structure is very similar to that of $Nd_2Fe_{14}B$ except that the boron sites are vacant. The Curie temperature, T_C, increases with a modest Al substitution in spite of little changes in the saturation magnetization M_s. However, both T_C and M_s decrease for a higher Al substitution. All the specimens have negative K_1 and positive K_2. The easy axis of magnetization is parallel to the [100] direction since $K_1+2K_2<0$ is satisfied for all the specimens. Although the magnitude of K_1+2K_2 decreases and becomes closer to zero with increasing Al content, aluminum substitution seems to be ineffective to change the easy direction from the basal plane to the c-axis.

Keywords: Crystal growth; Flux method; $Sm(Fe_{1-x}Al_x)_7$; Magnetic properties; Magnetic anisotropy

1. Introduction

Since the attainment of notable improvement in hard magnetic properties in the nitrogenated system of $Sm_2Fe_{17}N_x$ [1], which has a maximum energy product of 60 MGOe [2], the Sm–Fe system has been the focus of considerable attention and extensive studies. The Sm–Fe system appears to be promising with regard to finding new high-performance hard magnetic materials. In the Sm–Fe system, the existence of another metastable compound of $SmFe_7$ has been pointed out in studies of rapidly quenched polycrystalline specimens [3,4]. However, the precise properties of this compound were unclear because the separation of $SmFe_7$ phase was unsuccessful in this system. Recently, a single crystal of $SmFe_7$ was obtained by the self-flux method, and its crystallographic and magnetic properties have been characterized in detail [5,6]. $SmFe_7$ crystallizes in a tetragonal structure of the space group $P4_2/mnm$. This structure is similar to that of $Sm_2Fe_{14}B$; however, the boron sites in the crystal lattice of $Sm_2Fe_{14}B$ are vacant in the lattice of $SmFe_7$. The results of magnetization and magnetic torque measurements indicated that $SmFe_7$ has a significantly large spontaneous magnetization of 136 emu/g at 293 K, a large magnetocrystalline anisotropy constant K_1+K_2 of -6.9×10^7 erg/cc at 293 K, and a high Curie temperature T_C of 608 K. These properties are comparable to those of $Nd_2Fe_{14}B$, which is well known as a super-hard magnetic material [7–9]. $SmFe_7$ is a promising material for high-performance hard magnets.

In spite of its excellent properties, $SmFe_7$ has a serious drawback for practical use as a hard magnetic material because the easy magnetization direction is in the (001) plane. Therefore, further improvement in hard magnetic properties is necessary to make $SmFe_7$ a practical material. It is well known that the hard magnetic properties of intermetallic compounds which consist of rare-earth and transition metal elements are often considerably improved by substituting non-magnetic elements such as B, Al, and N. In particular, it is well known that the spontaneous magnetization, Curie temperature, and magnetocrystalline anisotropy of R_2Fe_{17} (R=Nd, Sm) are significantly improved by substituting aluminum into the Fe sites [10,11]. In this study, in order to improve hard magnetic properties, we investigated the effect of Al substitution on the magnetic properties of $SmFe_7$. This paper presents the results of crystallographic and magnetic measurements

*Corresponding author.
E-mail address: ynag@ee.aoyama.ac.jp (Y. Nagata).

0925-8388/00/$ – see front matter
PII: S0925-8388(00)01104-X

performed for single-crystalline specimens of $Sm(Fe_{1-x}Al_x)_7$.

2. Experimental

Single crystals were grown by the self-flux method. Excess Sm was used as a flux. After melting Sm (99.9%), Fe (99.9%), and Al (99.9%) in an atomic ratio of Sm:(Fe+Al)=6:4 in an arc furnace in an Ar atmosphere, the mixture was placed in BN-coated alumina. The crucible was sealed in a quartz ampoule with back-filled Ar gas of 460 Torr in order to prevent the evaporation of Sm. A zirconium oxygen getter was also placed in the ampoule. The mixture was heated to 1000°C in an electric furnace, and, after being held at that temperature for 6 h, it was cooled from 1000 to 800°C at a rate of 1°C/h. After the slow cooling was completed, the mixture was cooled to room temperature. The crystals were removed mechanically from the Sm flux.

The chemical composition of the crystal was determined by electron-probe microanalysis (EPMA) using wavelength dispersive spectrometers. The crystal structure was characterized by using single-crystal X-ray diffraction with a 4-circle-goniometer and X-ray powder diffraction. Refinement of the crystal structure was performed by the Reitveld method for X-ray diffraction data. The crystallographic directions were determined by the X-ray Laue back-reflection method. Magnetization measurements were performed by means of a vibrating sample magnetometer (VSM) and a SQUID magnetometer at temperatures from 5 to 800 K in applied magnetic fields up to 50 kOe. Magnetic anisotropy was characterized by means of magnetization measurements.

3. Results and discussion

3.1. Crystal growth and crystallographic properties

Freestanding rectangular parallelepiped crystals were grown on the surface of the flux, which remained at the bottom of the crucible. Since the Sm-flux was easily oxidized in the ambient atmosphere and changed to powder, the crystals could be readily removed from the flux. The crystals had smooth surfaces and metallic luster. The maximum size of the crystal was about $1\times1\times0.5$ mm^3. Although it was not a simple task to control the composition of Al, crystals with compositions of $Sm(Fe_{1-x}Al_x)_7$ (x=0, 0.047, 0.07 and 0.12) were grown. Fig. 1 shows the X-ray powder diffraction profile of the crystals with x=0.047. The diffraction profiles of the crystals have the same characteristics as those of $SmFe_7$ [9]. The diffraction data of all the crystals could be refined assuming a tetragonal structure of space group $P4_2/mnm$. The results of the refinement indicated that Al occupies Fe sites. The tetragonal lattice constants obtained by the refinement are shown in Fig. 2 as a function of Al content

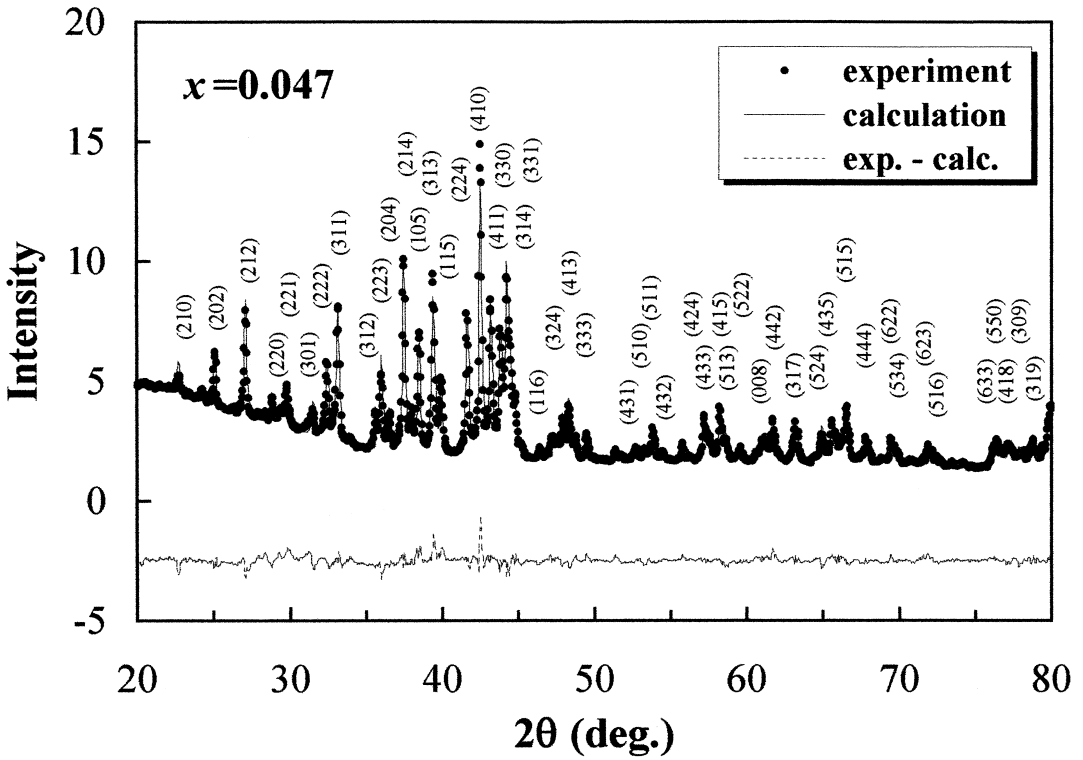

Fig. 1. X-ray powder diffraction profile of a crystal with x=0.047.

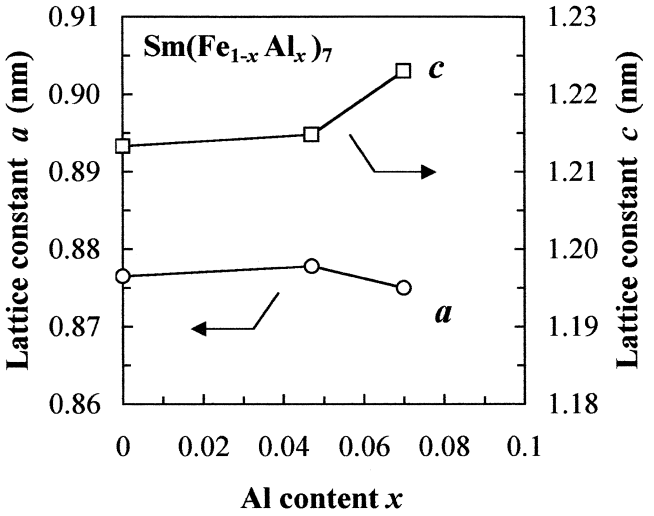

Fig. 2. Refined tetragonal lattice constants of $Sm(Fe_{1-x}Al_x)_7$ as a function of Al content x.

x. Lattice constant a is only slightly composition dependent. However, lattice constant c shows a monotonous increase with Al substitution. In general, the metallic bond radius of Al (0.143 nm) is larger than that of Fe (0.124 nm) [12]. Therefore, the crystal lattice of $SmFe_7$ must be expanded by Al substitution. This seems to be a reason of the increase in the c constant. However, the reason why the lattice expands only along the c-axis is not clear at present.

3.2. Magnetic properties

Magnetic properties were measured for disk-shaped single-crystalline specimens. The disk-plane of the specimens is parallel to the (001) plane. In the magnetization measurements at temperatures above 300 K, specimens were sealed in a quartz tube after being evacuated at 1×10^{-5} Torr to prevent oxidation and decomposition of the specimen at higher temperatures. The temperature dependence of magnetization was measured for specimens with $x=0$, 0.047 and 0.12 under a magnetic field of 10 Oe applied parallel to the [100] axis. $M(T)$ for a specimen with $x=0.047$ is shown in Fig. 3 as an example. The inset of Fig. 3 shows the temperature derivative of the magnetization. From the dip observed in the temperature dependence of dM/dT, the Curie temperature of the specimens was determined. The composition dependence of Curie temperature T_C is shown in Fig. 4. T_C is increased by substituting of a small amount of Al; however, after showing a small maximum, T_C tends to decrease as the Al content increases. This behavior is similar to that observed in the study of $Sm_2Fe_{17-x}Al_x$ [10,11]. It is well accepted that the Curie temperature of compounds that consist of rare earth (R) and transition metal (TM) depends on the exchange interaction between TM atoms and increases in accordance with the increase in the atomic distance

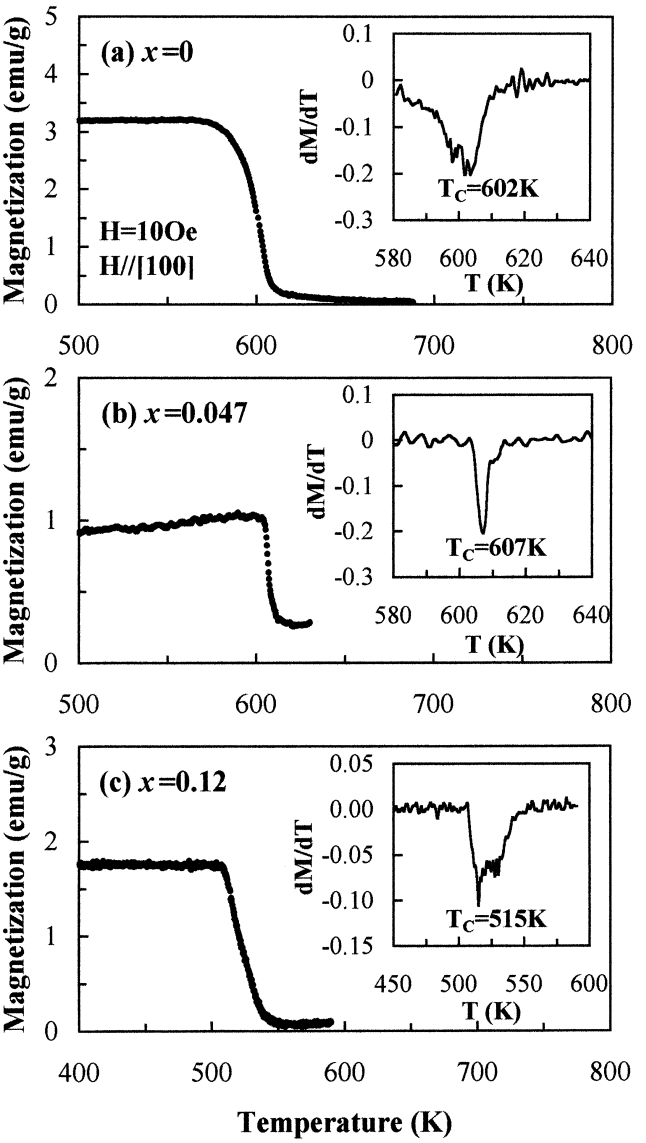

Fig. 3. Temperature dependence of magnetization measured for a specimen with (a) $x=0$, (b) $x=0.047$ and (c) $x=0.12$ under a magnetic field of 10 Oe applied parallel to the [100] axis. The inset shows the temperature dependence of the temperature derivative of the magnetization.

between TM atoms. It was shown in the previous section that the lattice volume is expanded (or lattice constant c increases) by substituting with a small amount of Al. The increase in T_C, which was observed for samples with an Al content of $x\leq0.07$, may be attributed to the increase in the atomic distance of Fe atoms. However, further Al substitution will decrease T_C because of a reduction in the number of Fe–Fe interactions.

Fig. 5a shows the magnetic-field dependence of magnetization measured for specimens with $x=0$, 0.047, and 0.12 at 5 K by applying a magnetic field parallel to the three principal directions, [100], [110] and [001]. The magnetization of all the specimens tends to saturate at a low magnetic field in the [100] direction, while magnetization could not be saturated up to 50 kOe in the [001]

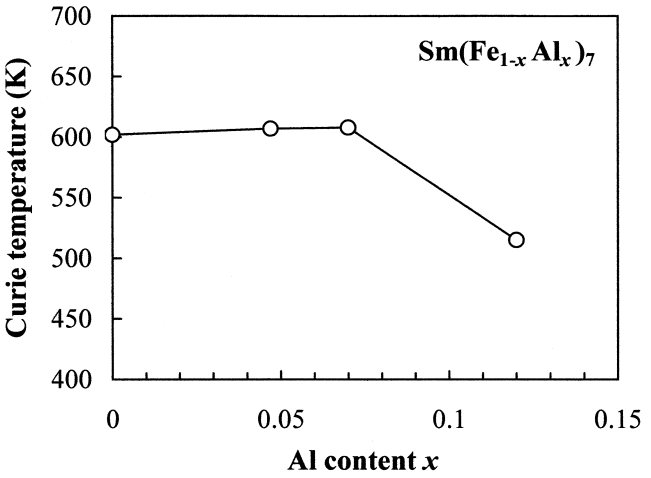

Fig. 4. Composition dependence of the Curie temperature, T_C.

direction, suggesting the existence of a large anisotropy field. These results indicate that the easy and hard directions of magnetization are parallel to the [100] and [001] directions, respectively. Magnetization measured for the same specimens at 300 K in the magnetic field applied parallel to the three principal directions is shown in Fig. 5b as a function of the magnetic field. It can be seen that the easy and hard axes of magnetization are in the same directions as those at 5 K. Fig. 6 shows the Al content dependence of the saturation magnetization determined from $M(H)$ in the [100] direction at 5 K and 300 K. The saturation magnetization at 5 K and 300 K decreases as the Al content increases. This would be due to the magnetic dilution caused by substituting non-magnetic Al. Fig. 7 shows the angular dependence of magnetization measured for specimens with $x=0$, 0.047 and 0.12 in the (100) and (001) planes under a magnetic field of 10 kOe at 300 K. The $M(\theta)$ of all the specimens shows almost the same behavior, and maximum and minimum magnetization are observed when the magnetic field is applied to the [100] and [001] directions, respectively, reflecting the tetragonal symmetry of the crystals. These results indicate that the easy and hard directions of magnetization are in the [100] and [001] directions, respectively.

Fig. 8 shows the temperature dependence of magnetization measured for specimens of $x=0$, 0.047 and 0.12

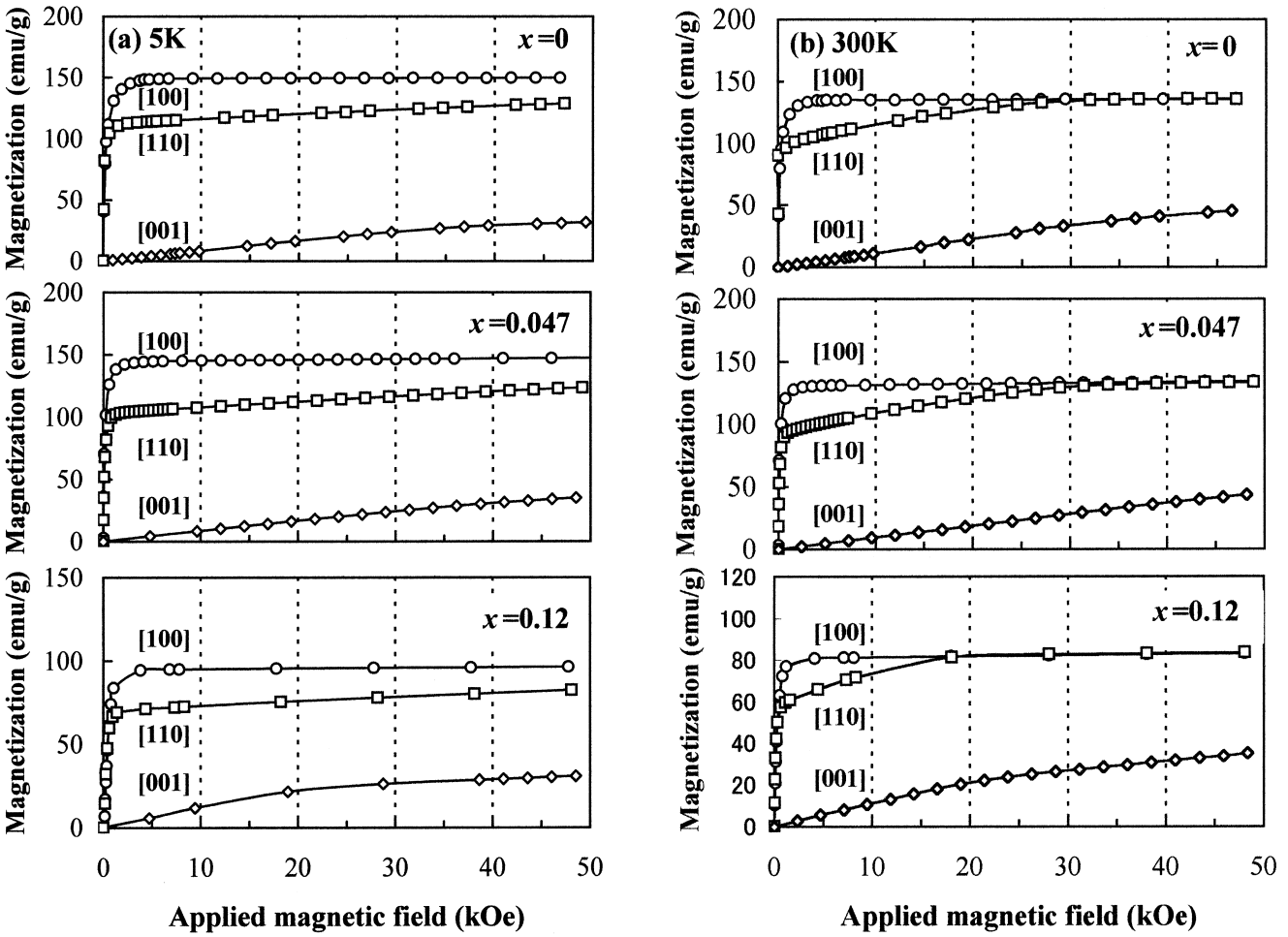

Fig. 5. Magnetic-field dependence of magnetization measured for specimens with $x=0$, 0.047, and 0.12 at (a) 5 K and (b) 300 K by applying a magnetic field parallel to the three principal directions of [100], [110] and [001].

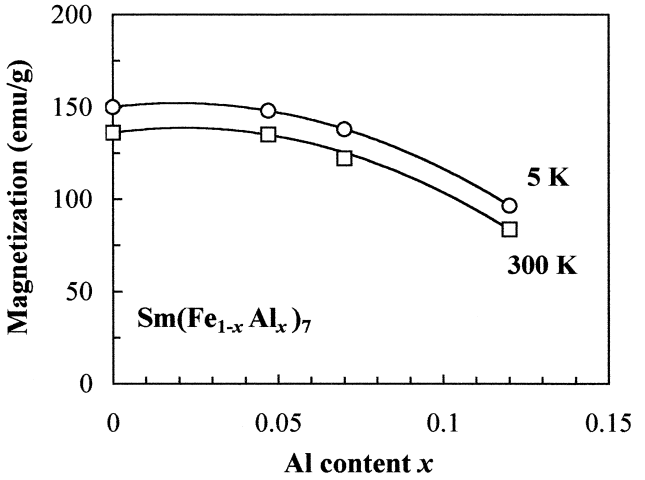

Fig. 6. Al content dependence of saturation magnetization M_s. M_s was determined from the $M(H)$ curve in the [100] direction at 5 K and 300 K.

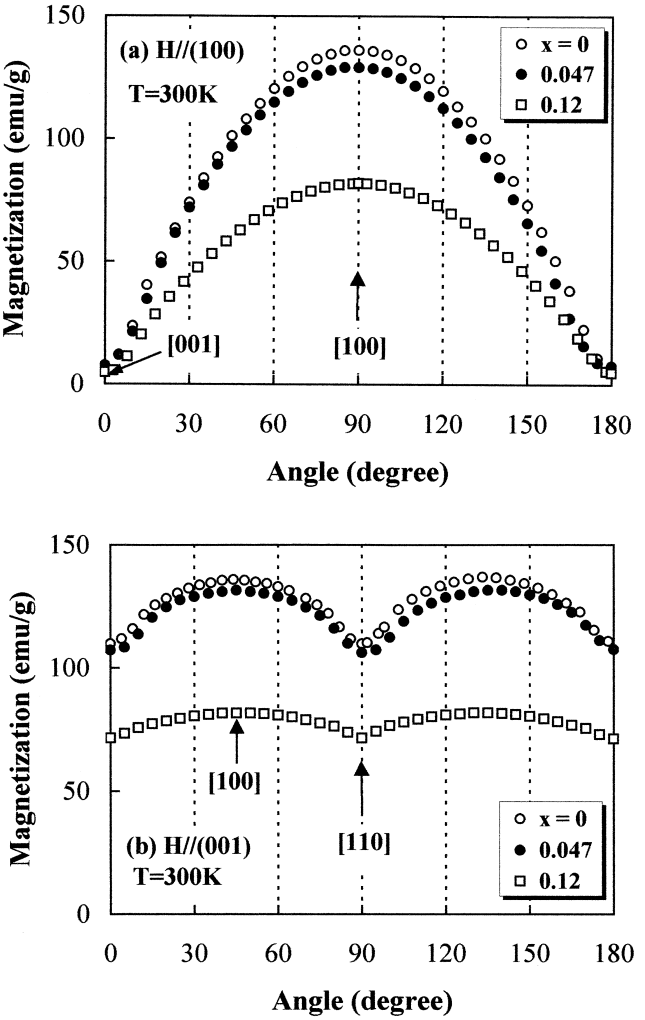

Fig. 7. Angular dependence of magnetization measured for specimens with $x=0$, 0.047 and 0.12 in the (a) (100) and (b) (001) planes under a magnetic field of 10 kOe at 300 K.

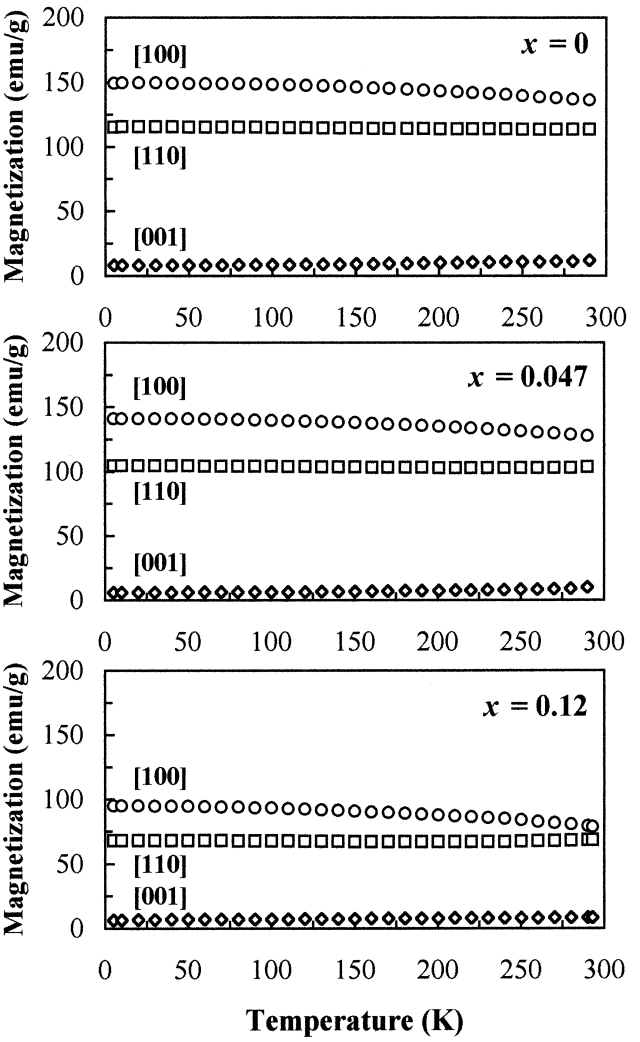

Fig. 8. Temperature dependence of magnetization measured for specimens of $x=0$, 0.047 and 0.12 under a magnetic field of 10 kOe applied parallel to the [100], [110] and [001] directions.

under a magnetic field of 10 kOe applied parallel to the [100], [110] and [001] directions. Magnetization in the [100] direction tends to decrease for all the specimens with increasing temperature, while there is little change in the magnetization in other directions. The magnitude of magnetization in each direction is always in the sequence $M_{100} > M_{110} \gg M_{001}$, where M_{100}, M_{110} and M_{001} are the magnetization in the [100], [110] and [001] directions, respectively. This suggests that the easy direction of magnetization is always in the [100] direction and does not change at temperatures between 5 K and 300 K. Fig. 9 shows coercive field ${}_{M}H_c$ determined from $M(H)$ curves measured for specimens of $x=0$, 0.047 and 0.12 in the [110] direction at 5 K. The coercive field ${}_{M}H_c$ increases with A1 substitution. This may be due to an enhancement of the anisotropy field or a pinning of the magnetic domain wall by centers introduced by Al substitution. However, the exact reason of the increase in ${}_{M}H_c$ is not clear at the present stage.

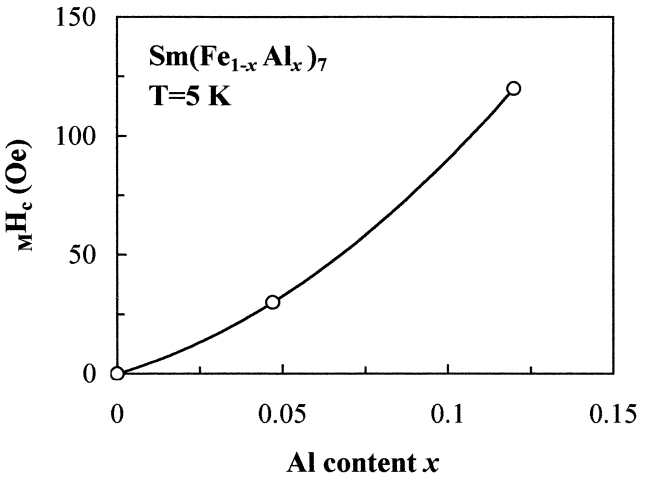

Fig. 9. Al content dependence of coercive field ${}_{M}H_{c}$ measured in the [110] direction at 5 K.

3.3. Magnetocrystalline anisotropy

The effect of Al substitution on the anisotropy of $SmFe_7$ was investigated by means of magnetization measurements. In general, the magnetocrystalline anisotropy energy of a tetragonal crystal is represented by

$$E_a = K_0 + K_1 \sin^2\theta + K_2\sin^4\theta + K_3\sin^4\theta \cos 4\varphi \quad (1)$$

where K_i ($i = 0$–3), θ and φ are the tetragonal anisotropy constants, the angle between the [001] direction and spontaneous magnetization M_s, and the angle between the [100] direction and M_s, respectively. When the anisotropy in the (001) plane (*ab* plane) is very small, the E_a is given by

$$E_a = K_0 + K_1\sin^2\theta + K_2\sin^4\theta \quad (2)$$

In an applied magnetic field H, the total energy E of the system is given by the sum of the Zeeman energy and the anisotropy energy denoted by Eq. (2) and is then expressed as $E = -M_s \cdot H + E_a$, where $-M_s \cdot H$ is Zeeman energy. When the spontaneous magnetization M_s lies at an angle θ from the [001] direction, the magnetization M observed in the [001] direction is given by $M = M_s\cos\theta$, and E is further expressed by

$$E = -M_sH\cos\theta + K_0 + K_1\sin^2\theta + K_2\sin^4\theta \quad (3)$$

At the equilibrium state, M_s lies in a direction where $\partial E/\partial\theta = 0$ is satisfied, and, in this case, the formula

$$M_sH\sin\theta + 2K_1\sin\theta\cos\theta + 4K_2\sin^3\theta\cos\theta = 0 \quad (4)$$

is derived. When $\cos\theta = M/M_s$ is substituted into Eq. (4), the relation

$$\frac{H}{M} = \left(\frac{4K_2}{M_s^4}\right)M^2 - \frac{2K_1 + 4K_2}{M_s^2} \quad (5)$$

is obtained. This formula indicates that when the magnetization curve is measured along the [001] direction and H/M is plotted as a function of M^2, the H/M has linear M^2 dependence [13]. Therefore, the slope and the ordinate intercept of the straight line fitted to the data at larger M^2 give $4K_2/M_s^4$ and $-(2K_1+4K_2)/M_s^2$, respectively, and then the anisotropy constants K_1 and K_2 can be calculated using saturation magnetization M_s obtained by magnetization measurements. The magnetocrystalline anisotropy constants K_1 and K_2 determined by magnetization measurements are shown in Fig. 10 as a function of Al content x. The magnitude of both K_1 and K_2 increases when a small amount of Al is substituted for Fe. However, it decreases with further Al substitution. It is well accepted that the easy direction of magnetization of the tetragonal crystal is determined by K_1+2K_2 when $K_1<0$. When $K_1+2K_2<0$ is satisfied, the easy direction lies in the (001) plane (or c plane), while when $K_1+2K_2>0$, the easy direction lies on the surface of a cone with a half-cone angle θ from the c-axis, where θ is represented by $\theta = \sin^{-1}(-K_1/2K_2)^{1/2}$. As shown in Fig. 10, K_1+2K_2 has negative values for all the specimens investigated in this study, indicating that the easy direction of magnetization lies in the (001) plane (or basal plane). This is consistent with the results of magnetization measurements. In general, the magnetocrystalline anisotropy of rare earth compounds is influenced by the configuration of the 4f-orbital of the rare-earth ion (hereafter referred to as R^{3+}), and the configuration of the orbital is determined by the geometric configuration of ligand R^{3+} ions. In the crystal lattice of $SmFe_7$, the lattice spacing among R^{3+} ($=Sm^{3+}$) ions in the (001) plane is shorter than that in the [001] direction. Therefore, the long axis of the cigar-like 4f-orbital of Sm^{3+} would be fixed in the (001) plane by the crystal field of ligands. Since the magnetic moment of Sm^{3+} is parallel to the long axis of the 4f orbital, the magnetic moment of Sm^{3+} must be parallel to the (001) plane. The magnetic

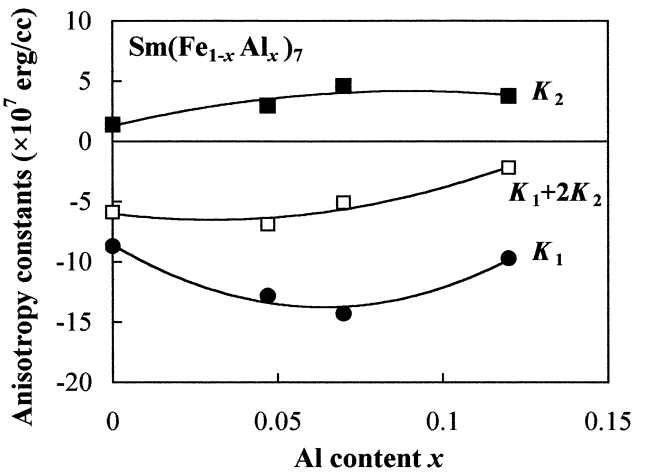

Fig. 10. Al content dependence of magnetocrystalline anisotropy constants K_1, K_2, and K_1+2K_2 determined by magnetization measurements at 300 K.

moment of iron interacts with the moment of Sm^{3+} and then aligns along the direction of the Sm^{3+} moment. This may explain why the spontaneous magnetization of $SmFe_7$ lies in the (001) plane. The magnitude of K_1+2K_2 decreases with a higher Al substitution and becomes closer to zero. Therefore, for further Al substitution, the sign of K_1+2K_2 may change to positive, and the easy direction of magnetization may tilt out of the basal plane.

4. Conclusion

$Sm(Fe_{1-x}Al_x)_7$ ($x=0$, 0.047, 0.07 and 0.12) crystals were grown by the self-flux method, and their crystallographic and magnetic properties were studied. $SmFe_{7-x}Al_x$ has a tetragonal structure of the space group $P4_2/mnm$, and aluminum substitutes into the iron site. This structure has a remarkable resemblance to that of $Nd_2Fe_{14}B$ except that the boron sites are vacant. The Curie temperature, T_C, increases for low Al substitution in spite of there being little change in saturation magnetization M_s. However, both T_C and M_s decrease for a higher Al substitution. All the specimens have negative K_1 and positive K_2 and satisfy $K_1+2K_2<0$. Therefore, the easy axis of magnetization is parallel to the [100] direction. Although the magnitude of K_1+2K_2 decreases and becomes closer to zero with the increasing Al content, substituting aluminum seems to be ineffective to change the easy axis from the basal plane to the c-axis.

Acknowledgements

Research performed at Aoyama Gakuin University was supported by The Science Research Fund of the Japan Private School Promotion Foundation and a Grant-in-Aid for Scientific Research from the Ministry of Education, Science, Sports and Culture, Japan.

References

[1] J.M.D. Coey, H. Sun, J. Magn. Magn. Mater. 87 (1990) 251.
[2] T. Iriyama, K. Kobayashi, N. Imaoka, T. Fukuda, H. Kato, Y. Nakagawa, IEEE Trans. Magn. 28 (1992) 2326.
[3] H. Hiroyoshi, H. Yamauchi, Y. Yamaguchi, H. Yamamoto, Y. Nakagawa, M. Sagawa, Solid State Commun. 54 (1985) 41.
[4] O. Mao, J. Yang, Z. Altounian, J.O. Strom-Olsen, J. Appl. Phys. 79 (1996) 4609.
[5] H. Samata, Y. Satoh, Y. Nagata, T. Uchida, M. Kai, M.D. Lan, Jpn. J. Appl. Phys. 36 (1997) L476.
[6] H. Samata, N. Fujiwara, Y. Nagata, T. Uchida, M.D. Lan, Jpn. J. Appl. Phys. 37 (1998) 3290.
[7] M. Sagawa, S. Fujimura, H. Yamamoto, Y. Matsuura, S. Hirosawa, J. Appl. Phys. 57 (1985) 4094.
[8] H. Hiroyoshi, H. Yamauchi, Y. Yamaguchi, H. Yamamoto, Y. Nakagawa, M. Sagawa, Solid State Commun. 54 (1985) 41.
[9] H. Yamauchi, M. Yamada, Y. Yamaguchi, H. Yamamoto, S. Hirosawa, M. Sagawa, J. Magn. Magn. Mater. 54–57 (1986) 575.
[10] H. Kato, J. Shiomi, T. Koide, T. Iriyama, M. Yamada, Y. Nakagawa, J. Alloys Compd. 222 (1995) 62.
[11] Fu-ming Yang, Xin-wen Li, N. Tang, Jian-li Wang, Lu Zhong-hua, Tong-yun Zhao, Qing-an Li, J.P. Liu, F.R. de Boer, J. Alloys Compd. 221 (1995) 248.
[12] L. Pauling, in: The Nature of the Chemical Bond, Cornell Univ. Press, New York, 1960, p. 256.
[13] W. Sucksmith, J.E. Thompson, Proc. Roy. Soc. A225 (1954) 362.